

1 **A sudden increase in the concentration of dissolved organic carbon in precipitation at a**
2 **northeastern US forest**

3

4 Mark B. Green^{1,2}, John L. Campbell², Danielle K. Hare³, Garrett Higgins⁴, Armistead G. Rus-
5 sell⁵, Christopher T. Solomon³, Charles T. Driscoll⁶

6

7 ¹ Case Western Reserve University, Department of Earth, Environmental, and Planetary Sci-
8 ences, Cleveland, Ohio

9 ² USDA Forest Service, Northern Research Station, Durham, New Hampshire

10 ³ Cary Institute of Ecosystem Studies, Millbrook, New York

11 ⁴ Hubbard Brook Research Foundation, Woodstock, Vermont

12 ⁵ Georgia Institute of Technology, School of Civil and Environmental Engineering, Atlanta,
13 Georgia

14 ⁶ Syracuse University, Department of Civil and Environmental Engineering, Syracuse, New
15 York

16

17

18

19 **Abstract**

20 The oxidation of organic matter from fuel combustion or vegetation emissions into organic acids
21 is a major source of dissolved organic carbon (DOC) in precipitation. Long-term measurements
22 of DOC in precipitation are rare, but the existing records mostly show decreases due to reduction
23 in fuel combustion. Here, we show a recent, sudden increase in precipitation DOC concentration
24 in a 27-year record from the Hubbard Brook Experimental Forest (HBEF) in northern New
25 Hampshire, U.S.A. Starting in 2010, mean annual DOC concentration increased from about 80 to
26 130 $\mu\text{mol L}^{-1}$ in 2022. No other solutes in precipitation showed a similar, sudden change. The
27 weekly DOC concentration was not clearly related to the 72-hour air mass trajectory characteris-
28 tics or changes in trajectories. We assessed the feasibility of multiple possible causes for the
29 DOC increase, including an increase in biogenic volatile organic compound (BVOC) emissions
30 from the forest or from forest fires, changes in oxidation processes in the troposphere, and

31 changes in gas-phase solubility due to increasing pH in precipitation. Further study of sudden
32 changes in BVOC emissions in the region, possible causes and air quality effects are warranted.

33

34 Key Points

35 • Dissolved organic carbon (DOC) in bulk deposition drastically increased over the recent
36 decade at a long-term research forest.

37 • The cation-to-anion charge balance suggested the presence of an unmeasured anion,
38 indicating that the DOC could come from organic acids.

39 • Possible causes of the DOC increase include enhanced biogenic volatile organic
40 compound emissions or their oxidation and dissolution.

41 Introduction

42 Organic carbon (OC) in the atmosphere is common and can play an important role in tropo-
43 spheric chemistry (Heald et al. 2008, Heald and Kroll 2020) and precipitation formation pro-
44 cesses (Yu 2000, Sun and Ariya 2006). The primary sources of OC are emissions from fossil fuel
45 combustion, biomass burning, and the production of biogenic volatile organic compounds
46 (BVOCs) emitted from plants and soils (e.g., Saarikoski et al. 2008, Sindelarova et al. 2014, US
47 EPA 2023). Emissions of OC can undergo oxidation by reactions with O₃, the OH radical, NO_x
48 or SO₂ resulting in new secondary OC species. In particular the OH radical associated with OC
49 play a major role in determining the oxidation potential of the atmosphere (Lelieveld et al. 2016).
50 Products from the oxidation of BVOCs include organic acids (Link et al. 2021), which can be
51 scavenged by precipitation and become a large source of dissolved organic carbon (DOC) in at-
52 mospheric deposition (Iavorivska et al. 2016). Organic acids have long been recognized as an
53 important source of anions in precipitation (Likens et al. 1983).

54

55 The amount of DOC in precipitation is typically small relative to other parts of terrestrial ecosys-
56 tem carbon budgets (e.g., Fahey et al. 2005). Atmospheric deposition of DOC ranges from 7.7 to
57 34 kg C ha⁻¹ yr⁻¹ (Liptzin et al. 2022) compared to ecosystem gross primary productivity and res-
58piration fluxes on the order of thousands of kg ha⁻¹ yr⁻¹ (Zheng et al. 2020, Tagesson et al. 2024).
59 Concentrations of dissolved organic carbon in precipitation tend to be higher in the tropics and
60 lower in northern latitudes, and concentrations over the ocean are lower than on terrestrial
61 sources (Liptzin et al. 2022). Although the amount of DOC in precipitation is small relative to
62 other ecosystem carbon fluxes, changes in precipitation DOC concentrations may provide insight
63 into changing atmospheric and ecosystem processes.

64

65 Few long-term records of atmospheric DOC deposition exist (Liptzin et al. 2022). National net-
66 works of atmospheric deposition do not include DOC as a routinely analyzed solute (Lamb and
67 Bowersox 2000). The trends at individual sites reported by Liptzin et al. (2022) showed some
68 trends in DOC concentration over time, which were mostly declines, likely associated with de-
69 creasing fuel combustion. A site in the northeastern U.S. has shown increasing total OC in at-
70 mospheric deposition (Lawrence et al. 2023). One of the longest-running datasets of DOC in pre-

71 cipitation in the United States is from the Hubbard Brook Experimental Forest in New Hamp-
72 shire, where weekly measurements have been made at one bulk deposition station since 1995,
73 and two additional stations since 2013 (HBWatER 2023). In this study we evaluate trends in
74 DOC bulk deposition and examine other constituents in precipitation that may provide insight
75 into long-term changes in atmospheric chemistry or forest ecosystem processes.

76

77 **Methods**

78

79 Site Description

80 The Hubbard Brook Experimental Forest (HBEF) is a 3500-ha research reserve in the White
81 Mountains of central New Hampshire in the northeastern U.S. (43°56'N, 71°45'W). The climate
82 at the site is cool, humid, and continental; the mean minimum daily temperature in January is -9
83 °C and the mean maximum daily temperature in July is 18 °C (Campbell et al. 2021). Mean an-
84 nual precipitation is 1400 mm which is distributed evenly throughout the year. About a third of
85 precipitation falls as snow, and there is typically a continuous snowpack that on average persists
86 from late December until mid-April. The forest cover type is predominantly northern hardwood
87 (sugar maple (*Acer saccharum*)), American beech (*Fagus grandifolia*), and yellow birch (*Betula*
88 *alleghaniensis*)), with some spruce-fir (red spruce (*Picea rubens*) and balsam fir (*Abies bal-*
89 *samea*)) at higher elevations.

90

91 Sample Collection and Handling

92 Concentrations of major solutes in precipitation have been monitored at the HBEF since 1963
93 (HBWatER 2024). Analysis of DOC in precipitation started later, beginning in 1995 at one loca-
94 tion on a south-facing slope and in 2013 at two additional locations: one on a north-facing slope
95 (RG23) and the other at the US Forest Service headquarters building (RG22). In this analysis, we
96 used the portion of the chemistry record when DOC data were available (1995-2022). In 2017,
97 precipitation chemistry sampling on the south-facing slope was moved from RG11 to RG1, a dis-
98 tance of 811 m. A comparison of major solutes between the two collectors indicated no signifi-
99 cant difference (Buso 2000). All chemistry collectors used in this study are within 7 km of each
100 other and range in elevation from 255-668 m.

101

102 At the HBEF, precipitation samples for chemical analysis are collected weekly in bulk collectors
103 that are continuously open to the atmosphere (see Buso et al. 2000). Chemical concentrations ob-
104 tained from bulk collectors are comparable to concentrations from a wet-only collector associ-
105 ated with the National Trends Network (<https://nadp.slh.wisc.edu/networks/national-trends-network/>) based on an analysis of major solutes at the HBEF (Martin et al. 2000), however analysis
106 of DOC was not included in this comparison. The bulk collector used during the warmer months,
107 when precipitation falls mostly as rain, consists of a high-density polyethylene (HDPE) funnel
108 connected by tubing to a sample bottle housed in a container that shields sample water from sun-
109 light. The tubing has a loop that partially fills with water and serves as a vapor barrier to mini-
110 mize evaporation. A plug of acid-washed polyfill is placed in the neck of the funnel to keep de-
111 bris out of the sample bottle. During winter, when precipitation falls mostly as snow, samples for
112 precipitation chemistry are collected with an open-top HDPE bucket. Samples containing frozen
113 water are brought to the lab, melted at room temperature, and poured into bottles for chemical
114 analysis. Thus, each sample is frozen for less than one week before it is retrieved from the field.
115 Both types of collectors deployed in the field are replaced weekly with collectors that have been
116 cleaned and acid washed.

118

119 Precipitation chemistry collectors are collocated with weight-recording rain gages for measuring
120 precipitation volume (USDA Forest Service 2024). The chemistry collectors and rain gages are
121 mounted 2 m above the ground in a clearing where vegetation is removed approximately every 3
122 years so that no portion of the surrounding canopy intersects a 45-degree angle from the rims up-
123 ward (Buso et al. 2000). The resulting vegetation in the clearing is dominated by raspberry
124 (*Rubus ideaus*) and hayscented fern (*Dennstaedtia punctilobula*), which are also major under-
125 story species that emerge after forest disturbance at the HBEF (Hughes and Fahey 1991). Precip-
126 itation volume was measured with a mechanical Belfort Universal Precipitation Gage (5-780
127 model) until 2011, when it was replaced with an electronic, ETI Instruments rain gage (NOAH
128 IV model). The older rain gage model produced a continuous record of precipitation on a strip
129 chart that was collected weekly. These strip charts were recently digitized to extract precipita-
130 tion volume at 15-minute intervals, which matches the interval of the new, electronic gage to
131 provide a complete record of 15-minute data.

132

133 Chemical analyses were performed at the U.S. Forest Service Laboratory in Durham, New
134 Hampshire, except for pH, which was measured with a benchtop pH meter (Thermo Scientific,
135 Orion 3-Star) at the Hubbard Brook Experimental Forest laboratory on the same day samples
136 were collected. Samples were filtered with a pre-combusted glass-fiber filter (0.7 μm nominal
137 pore size) and stored frozen prior to analysis, except for Ca^{2+} , Mg^{2+} , Na^+ , K^+ and Si , for which an
138 aliquot was poured off and refrigerated. Samples were analyzed for SO_4^{2-} , NO_3^- and Cl^- using ion
139 chromatography (Metrohm 761); NH_4^+ with automated colorimetry (SmartChem AQ2 Discrete
140 Analyzer); Ca^{2+} , Mg^{2+} , Na^+ , K^+ , and Si with inductively coupled plasma optical emission spec-
141 troscopy (Agilent 730); and DOC and total dissolved nitrogen (TDN) using high-temperature
142 catalytic oxidation (Shimadzu TOC-VCSH analyzer). The Ca, Mg, Na, and K measurements
143 were of dissolved elements, not the ions, however we assumed that they were in ionic form. Dis-
144 solved organic nitrogen (DON) was determined by subtracting NO_3^- and NH_4^+ from TDN. Filtra-
145 tion for DOC began on March 7, 2005. A comparison of 37 filtered and unfiltered samples dur-
146 ing 2005 showed that filtered samples were 6.7 $\mu\text{mol L}^{-1}$ higher on average; we report the unfil-
147 tered values as DOC in the current study. More detailed field and analytical procedures can be
148 found in Buso et al. (2000) and method quantification and detection limits are in USDA Forest
149 Service (2019). We use data from the National Atmospheric Deposition Program station at the
150 HBEF (site NH02) to compare the total cation-to-anion charge balance in wet deposition with
151 results from our bulk deposition samples (National Atmospheric Deposition Program, 2022).

152

153 Air Mass Trajectory Analysis

154 We used the National Oceanic and Atmospheric Administration (NOAA) Hybrid Single-Particle
155 Lagrangian Integrated Trajectory (HYSPLIT) model (Stein et al. 2015) to evaluate whether
156 changing weather patterns could explain the recent increase in DOC at the HBEF. The precipita-
157 tion chemistry collector on the south-facing slope was used as the endpoint to calculate 72-hour
158 backward trajectories for air masses 500 m above ground level, which is thought to be repre-
159 sentative of in-cloud processes and has been used in previous studies of atmospheric transport of
160 DOC (Mead et al. 2013, Siudek et al. 2015). Since precipitation for chemical analysis is col-
161 lected weekly at the HBEF, samples can include water from multiple storms. For this analysis,
162 we only evaluated weekly chemistry that was associated with one discrete storm so that we could
163 reliably match a DOC concentration with an air mass trajectory (n=351). An event was defined

164 as a period of continuous precipitation lasting for six or more hours and totaling at least 6.35 mm
165 (0.25 inch) of total precipitation. The event end-dates, to the nearest 15-minute interval, were
166 used to calculate the backward trajectory with the HYSPLIT model.

167

168 We performed a k-means cluster analysis to group HYSPLIT trajectories (Hartigan and Wong
169 1979, Cui et al. 2021). Independent variables were the latitude, longitude, and distance from the
170 HBEF for each hour in the 72-hour trajectory. The number of clusters was plotted against their
171 explained variance and the lowest number that corresponded to the optimal inflection point on
172 the plot determined the number used in the analysis. In this case, the optimal number of clusters
173 was five. We calculated the total trajectory distance traveled, and the distance over land and wa-
174 ter (ocean or freshwater) for each 72-hour trajectory using the *sf* and *lwgeom* packages in R
175 (Pebesma 2018, Pebesma 2021, Pebesma and Bivand 2023).

176

177 Statistical Analyses

178 The seasonality in DOC concentrations was assessed using ANOVA tests with Tukey HSD *post*
179 *hoc* tests. Data from the entire record were used to first assess which months were statistically
180 distinct from one another. The presence of trends in time series was quantified using the Kendall
181 test within the *cor.test()* function in base R. A breakpoint analysis of the DOC bulk deposition
182 concentration using the *segmented* package in R (Muggeo 2016) was used to identify when DOC
183 began increasing. This included a Davies test to determine whether there was a significant break-
184 point and if a breakpoint was indicated, the year when the breakpoint occurred was identified.
185 The data were separated into two groups, prior to and after that breakpoint, and then the differ-
186 ences between DOC concentrations in the two groups and across months were assessed using an
187 ANOVA with a Tukey HSD *post hoc* test. The difference in DOC concentration across the dif-
188 ferent air mass trajectory clusters was assessed with an ANOVA test.

189

190 Comparison of DOC Trends with Other Solutes and Atmospheric Variables

191 The time series of other solutes in bulk deposition, atmospheric water vapor pressure, ozone, and
192 reactive nitrogen (N; $\text{NO}_3^- + \text{NH}_4^+ + \text{HNO}_3$) dry deposition were compared with the DOC con-
193 centration time series to develop new hypotheses about mechanisms responsible for changes in
194 the DOC concentration. Average daily vapor pressure was calculated from air temperature and

195 relative humidity, which were measured with a Campbell Scientific Inc. 201 digital sensor at the
196 RG 22 site (USDA Forest Service 2023). Ozone was measured at a CASTNET site about 100 m
197 away from RG 22 using a continuous UV ozone analyzer (Bloomer et al. 2010). Dry deposition
198 of reactive N (sum of N in NO_3 , NH_4 , and HNO_3) was estimated by measuring reactive N con-
199 centration from filter packs and modeling deposition velocities (Clarke et al. 1997). The annual
200 average during April to October was calculated for each variable, since that was the period when
201 DOC concentration in precipitation was highest, exhibited the greatest long-term change, and
202 thus when we were most interested in other solute and environmental changes.

203

204 Calculating the Effect of pH on Organic Acid Solubility in Precipitation

205 The solubility of organic acids in precipitation is a function of pH, which could be important at
206 the HBEF since precipitation pH has markedly increased since the 1990s (Fuss et al. 2015). We
207 evaluated that effect using Henry's law for estimating the concentration of non-disassociated
208 aqueous organic acids:

209 (1) $[\text{HA}] = p k_{\text{H}}$

210 where $[\text{HA}]$ is the concentration of a non-disassociated organic acid (molar), p is the partial pres-
211 sure for the gas phase of that organic acid (atm), and k_{H} is the Henry constant for that organic
212 acid ($\text{mol L}^{-1} \text{ atm}^{-1}$). We estimated the disassociated aqueous organic acids using the equilibrium
213 constant (K_a) for an organic acid (HA):

214 (2) $K_a = [\text{H}^+][\text{A}^-]/[\text{HA}]$

215 where K_a is the equilibrium constant for the organic acid, $[\text{H}^+]$ is the concentration of the hydro-
216 gen ion, and $[\text{A}^-]$ is the concentration of the conjugate base. Combining the non-disassociated
217 and disassociated (rearrange equation 2 for A^-) components results in an equation for the total
218 aqueous concentration (C_{tot}):

219 (3) $C_{\text{tot}} = p k_{\text{H}} (1 + K_a/[\text{H}^+]).$

220 We used our measured volume weighted H^+ concentration in bulk deposition and assumed a K_a
221 of 1.74×10^{-5} M for acetic acid and 1.78×10^{-4} M for formic acid (Khare et al. 1999), at 25 °C, to
222 estimate the theoretical change in the concentration of organic acids in precipitation due to a
223 change in H^+ . We assumed no change in the partial pressure of the organic acid in the atmos-
224 phere since we were estimating the % change that was theoretically possible given a change in

225 H^+ . We calculated the theoretical change for acetic and formic acid since they are abundant in the
226 troposphere above forests (Link et al. 2020).

227

228

229 **Results**

230 Mean annual DOC concentration ranged around 50 to 80 $\mu\text{mol L}^{-1}$ from 1996 to 2012 with nota-
231 ble spikes in 2000 and 2004, followed by an increase to about 130 $\mu\text{mol L}^{-1}$ by 2018 and has re-
232 mained at that level through 2022 (Figure 1). The DOC concentration increase was similarly ob-
233 served in precipitation collected at the two other bulk deposition collectors. A breakpoint analy-
234 sis identified a significant change in slope of the DOC concentration time series in 2010 ($\pm \text{SE}$ of
235 1.4 years; Davies test $p=0.0001$). DOC concentration was negatively related to storm precipita-
236 tion amount in log-log space across all months (Figure 2).

237

238 The DOC concentration had strong seasonality with the highest concentrations in the summer,
239 peaking in August, and the lowest concentrations in the winter (Figure 3a). There are six statisti-
240 cally distinct month groupings of DOC concentrations. After the 2009 breakpoint in DOC con-
241 centration, most months had a higher average DOC concentration, however only August, Sep-
242 tember, and October were significantly higher at the $\alpha=0.05$ level (Figure 3b).

243

244 The air mass trajectories fell into clusters that were largely associated with the direction from
245 which they approached (Figure 4a). Trajectory clusters 1 through 5 had a median azimuth direc-
246 tion of 202° , 76° , 258° , 328° , and 295° , respectively. Trajectory clusters 1 through 5 had a me-
247 dian distance from the HBEF of 345, 814, 782, 781, and 1183 km, respectively. Thus, Cluster 2
248 was notable because it was a more easterly trajectory, and Clusters 1 and 5 are notable for being
249 substantially shorter and longer, respectively, than the other trajectory clusters. Clusters 3 and 4
250 were typical lengths but approached from the west and north, respectively. Even with clear dif-
251 ferences in the characteristics of each group, the ANOVA showed no difference in DOC concen-
252 tration among the clusters ($p=0.58$; Figure 4b). The DOC concentration was, however, negatively
253 related to air mass trajectory length and positively related to the fraction over land (Spearman
254 $\rho=-0.11$, $p=0.04$; and $\rho=0.14$, $p=0.01$, respectively).

255

256 Other solutes and atmospheric factors provided context for how atmospheric chemistry changed
257 during the past three decades. Acid anions (SO_4^{2-} and NO_3^-), NH_4^+ , and H^+ decreased over time
258 (Figure 5; Table 1). K^+ , Ca^{2+} , and Mg^{2+} were variable with no clear change during the DOC in-
259 crease. Na^+ and Cl^- increased significantly, although this increase was not as clear as the acid an-
260 ions. The molar $\text{Na}:\text{Cl}$ ratio was mostly around 0.8 except for an unexplained spike in 2013 that
261 declined in the subsequent two years. The molar DOC:DON ratio was around 20 prior to 2010
262 and then increased to around 40 thereafter. The anion:cation ratio (cations are Na^+ , K^+ , Ca^{2+} ,
263 NH_4^+ , H^+ , and Mg^{2+} ; anions are SO_4^{2-} , Cl^- , and NO_3^-) was within 10% of 1 prior to 2013, and
264 then suddenly decreased, demonstrating an approximately 25% anion deficit from 2013 onwards.
265 This change in the balance of cations and anions was also apparent in wet deposition collected at
266 the NADP network site, showing a more gradual change towards an unmeasured anion starting
267 around 2010 (Figure 6). Average April to October DOC concentration was significantly nega-
268 tively correlated with SO_4^{2-} and H^+ and positively correlated with Na^+ and Cl^- (Table 1). The cal-
269 culated changes in aqueous acetate and formate concentrations in precipitation suggested a 69%
270 and 122% increase between 2010 and 2022, respectively, given changes in H^+ . The concentration
271 of volume-weighted H^+ concentration over the April-October interval was 15.8 $\mu\text{mol/L}$ in 2010
272 and 6.8 $\mu\text{mol/L}$ in 2022. Other atmospheric factors that potentially could impact the oxidation of
273 BVOCs in the atmosphere showed notable changes. Water vapor pressure increased, while ozone
274 and dry N deposition decreased (Figure 7).

275

276 **Discussion**

277 The abrupt increase in bulk deposition DOC concentration at the HBEF was surprising and chal-
278 lenging to explain. The change in anion-cation balance after 2012 is coincident with the initiation
279 of the DOC increase and suggests that organic anions are an important component of precipita-
280 tion chemistry, presumably in the form of dissociated organic acids, which have been previously
281 recognized in atmospheric deposition at the HBEF (Likens et al. 1983) and other forested sites
282 (Schaefer et al. 1989, Williams and Melack 1991, Link et al. 2020). The measured anion-cation
283 balance after 2012 showed a discrepancy that accounted for ~25% of the total anions. If the un-
284 measured anions were derived from organic acids, the proportion would be similar to the 25-30%
285 of total anion composition from acetic and formic acid measured at a Sierra Nevada forested site

286 (Williams and Melack 1991). Below, we discuss different possible causes of the DOC concentra-
287 tion increase and their likelihood.

288

289 It is not clear whether our observed increase in DOC concentration is a local phenomenon or part
290 of a larger-scale change, since published data on trends in DOC atmospheric deposition are lim-
291 ited. Past studies that documented changes in atmospheric deposition of DOC have shown de-
292 creases, mostly associated with reduction in fossil fuel combustion (Willey et al. 2011, Cao et al.
293 2022, Liptzin et al. 2022). We do not think that the DOC increase at the HBEF is associated with
294 an increase in fossil fuel-related sources of organic carbon, since inorganic acid anions associ-
295 ated with fossil fuel combustion (e.g., SO_4^{2-} , NO_3^-) have substantially decreased over time. One
296 site in the northeastern U.S. has shown an increase in the concentration of total organic carbon
297 (TOC) in precipitation that is of similar timing and magnitude as the increase in DOC observed
298 at the HBEF (Lawrence et al. 2023). Lawrence and colleagues also show a change in the cation-
299 anion balance towards unmeasured anions, show that the TOC is a source of acids, and demon-
300 strate that regional smoke events have higher deposition of TOC, thus hypothesizing that their
301 trend could be driven by increasing fire activity in upwind areas. We do not think that an in-
302 crease in smoke deposition is the driver of our observed increase in DOC concentrations since
303 smoke tends to contain elevated concentrations of Ca^{2+} , K^+ , and NO_3^- , which have not increased
304 with DOC at the HBEF (Evans et al. 2021, Boyer et al. 2022). Further, a notable regional smoke
305 deposition event occurred during the summer of 2002, causing an increase in aerosol organic car-
306 bon and other elements including K^+ (DeBell et al. 2004), but did not cause a clear spike in our
307 measured DOC at the HBEF (Figures 1 and 5). We cannot fully exclude the hypothesis that fire
308 could impact our increase in DOC concentration since fires emit VOCs that can be transported
309 across North America (de Gouw et al. 2006, Ciccioli et al. 2014), which could increase DOC
310 while having a minimal impact on other solutes. Also, smoldering fires have lower K^+ concentra-
311 tions than flaming fires (Allen and Miguel 1995), so there are fire conditions that could result in
312 higher DOC without elevated inorganic analytes.

313

314 While smoke could be a source of the DOC increase, other possible sources of DOC can be con-
315 sidered unlikely causes of the DOC concentration increase because they contain other analytes
316 that would have also increased. Dust can be a source of DOC (de Vicente 2012). However dust is

317 a major source of Ca^{2+} in the atmosphere to the extent that it has caused regional increases in
318 Ca^{2+} deposition in the western U.S. (Brahney et al. 2013). Pollen can be a source of DOC (Rösel
319 et al. 2012), however it is also a source of phosphorus, nitrogen, and K^+ (Lee et al. 1996). Insects
320 could introduce DOC to the deposition collectors, but they contain other ions like Ca^{2+} that
321 would increase if they were the source of DOC (Dube et al. 2000).

322

323 We do not see evidence that the DOC concentration increase is associated with changes in rain-
324 out processes or air mass source area changes. Rainout of DOC is an important mechanism that
325 controls the concentration of DOC in precipitation (Iavorivska et al. 2016). However, precipita-
326 tion is increasing at the HBEF (Campbell et al. 2021), which would result in decreases in DOC
327 concentrations due to dilution or more frequent removal. As a result, we do not think that
328 changes in precipitation amount are the cause of the DOC concentration increase. Further, pre-
329 cipitation at the HBEF has increased gradually over the long-term, rather than a recent marked
330 increase like DOC concentration. The trajectory analysis suggests that the increase in DOC con-
331 centration over time is not due to atmospheric transport changes, since there is no clear differ-
332 ence in DOC concentrations between the trajectory clusters that we tested.

333

334 Biogenic VOCs are a source of DOC that would not result in increases other analytes in precipi-
335 tation and thus are a possible source of the observed increase in DOC concentration. BVOCs are
336 emitted into the atmosphere by many tree species (Harley et al. 1999, Helmig et al. 1999). Com-
337 mon BVOCs from temperate forests include isoprene and monoterpenes (Nguyen et al. 2015),
338 which are precursors to organic acids in the atmosphere (Link et al. 2021). The generation of
339 DOC from BVOCs involves dissolution of gaseous BVOCs or forming secondary organic aero-
340 sols and then wet-scavenging (Safieddine and Heald, 2017). The seasonality of DOC concentra-
341 tion that we observed is similar to the phenology of the forest canopy at the HBEF (Richardson
342 et al. 2006), and the long-term increase was mostly driven by increases during the late summer,
343 suggesting that the DOC increase could be related to an increase in BVOC production by the for-
344 est at the HBEF or the surrounding region. This pattern is consistent with previous studies that
345 have monitored DOC concentrations seasonally and attributed the seasonality of DOC deposition
346 to BVOC emissions from terrestrial ecosystems (Willey et al. 2000, Siudek et al. 2015). Further,
347 terrestrial ecosystems can contribute up to 80% of OC in precipitation based on isotopic evidence

348 (Raymond 2005). Organic acids in the troposphere above forests are generally derived from
349 BVOCs (Link et al. 2020) and thus it is likely that the seasonality and the increase of DOC is as-
350 sociated with BVOC production, oxidation to organic acids and peroxides, and rainout at the
351 HBEF. If the source of organic carbon is BVOCs, multiple studies have shown that local BVOC
352 emissions can result in local organic acid production (Nguyen et al. 2015). However, if BVOCs
353 are the source of the DOC it is not clear why their production would increase in a sustained man-
354 ner. We think that it is reasonable to hypothesize that the increase in DOC concentration at the
355 HBEF is related to increases in BVOCs, but further work is needed to test this hypothesis.

356

357 Whether there has been a change in BVOCs emissions or not, a change in tropospheric oxidation
358 dynamics could cause higher DOC in bulk deposition. Atmospheric oxidants such as O₃ and re-
359 active N have been decreasing over time at the HBEF, raising questions about whether the in-
360 crease in the DOC concentration in precipitation might be associated with a decrease in the oxi-
361 dation of BVOCs leading to an increase in organic acids and peroxides and ultimately DOC.
362 Ozone and nitrogen oxides are precursors of OH radical (Lelieveld et al. 2016), which is a major
363 oxidant of BVOCs into organic acids (Link et al. 2021). Atmospheric water vapor pressure also
364 increased, which could have a positive effect on BVOC oxidation (e.g., Anglada et al. 2017).
365 However, changes in these factors may not necessarily be evidence of a change in the OH radical
366 abundance in the atmosphere (and thus the oxidation potential) due to the relatively stable OH
367 abundance from OH recycling (Lelieveld et al. 2016). The oxidation of isoprene has been
368 demonstrated to occur in low N environments like the Amazon rainforest (Paulot et al. 2009) and
369 is a likely cause of high concentrations of organic acids over forests (Link et al. 2020). The path-
370 ways for BVOC oxidation in low NO_x environments can result in greater production of water-
371 soluble secondary aerosols (Shrivastava et al. 2017). Therefore, while there were significant
372 changes in variables that are OH sources, this might not result in a step change of the oxidation
373 potential of the lower troposphere at the HBEF that would result in a sudden, sustained increase
374 in DOC concentration.

375

376 Our calculated potential increase in aqueous acetate and formate in precipitation due to the de-
377 crease in H⁺ was similar in magnitude to the changes in DOC that we observed. This pattern sug-

378 gests that it is feasible that the increase in DOC is due to a change in the solubility of organic ac-
379 ids in the troposphere. Our calculations assumed no change in the partial pressure of acetic and
380 formic acid during this period, however, if there were a change, we would hypothesize that the
381 partial pressure would have increased, due to our hypothesis that BVOCs have increased. The
382 lack of change in DOC from 1990 to 2010 a period when H^+ in precipitation decreased consider-
383 able, however, challenges the suggestion that this increase is entirely due to decreased H^+ (Figure
384 5e).

385

386 If the increase in DOC concentration in bulk deposition is due to an increase in BVOC emis-
387 sions, we hypothesize that this response could be caused by an increase in forest photosynthesis
388 or a heat stress response. The rate of BVOC flux can be attributed to changes in internal leaf bio-
389 chemical processes in response to environmental stimuli or stressors (Lantz et al. 2019). Isoprene
390 is associated with photosynthesis, particularly signaling the production of compounds involved
391 in plant growth and stress tolerance (Monson et al. 2020); therefore, an increase in gross primary
392 productivity (GPP) of the forest would increase a local isoprene atmospheric flux (Guenther et
393 al. 2006). This increase would align well with two observations from the HBEF that have sug-
394 gested an increase in GPP beginning between 2010-2015: (1) increased evapotranspiration be-
395 yond what could be explained by atmospheric drying potential (Green et al. 2021), and (2) a sud-
396 den large increase in soil respiration (Mann et al. 2024, Possinger et al., 2025). Additional con-
397 siderations would include climatic stresses such as drought and heat (Ferracci et al. 2020). Shal-
398 low soil moisture has been declining at the HBEF (Green et al. 2021; Wilson et al. 2025), how-
399 ever, this condition has not likely been dry enough to cause persistent moisture stress. Plus, trees
400 at the HBEF can access water from deeper soil water when surface soil water availability de-
401 clines (Harrison et al. 2020). The rate of air temperature increase has increased considerably in
402 late summer and early autumn months at the HBEF (Supplemental Figure 1), potentially increas-
403 ing heat stress on trees might be the cause of increases in BVOC emissions and DOC concentra-
404 tion in precipitation. The July summer air temperature at the HBEF increased from about 18°C in
405 2010 to about 20°C in 2022, which would result in a 22% increase in BVOC emissions accord-
406 ing to the McKinney et al. (2011) model of the temperature dependence of monoterpene emis-
407 sions at Harvard Forest in Massachusetts. This pattern suggests that the temperature effect would
408 not produce a large enough increase in monoterpene emissions to result in a doubling of DOC as

409 observed without some other mechanism in play, such as the increase in organic matter solubil-
410 ity.

411

412 Mechanical stresses such as herbivory or pest damage can stimulate BVOC plant-atmospheric
413 fluxes (Ghimire et al. 2022) and thus should be considered as playing a role in the increase in
414 DOC deposition at the HBEF. There was a high wind event in 2013 that damaged the forest can-
415 opy in areas of the HBEF (Battles et al. 2017); however the forest damage was concentrated in
416 specific areas of the HBEF valley. We observed the sustained increase in DOC concentration in
417 all three collectors that included one at the head of the valley that was 4 km from the concen-
418 trated forest damage. We are not aware of any sustained, valley-wide mechanical stress that
419 started at the HBEF in the 2010-2015 period. An increase of BVOC emissions can result from
420 changes in forest composition (Harley et al. 1999), leaf anatomy (Schollert et al. 2015), or leaf
421 age (Baldocchi et al. 1995), but changes in BVOC emissions associated with these would happen
422 gradually.

423

424 Additional research is needed to understand the cause of the increase in DOC concentration at
425 the HBEF and whether this is part of a larger scale phenomenon. Future measurements of or-
426 ganic anions in bulk deposition are needed to understand the composition of the DOC. Detailed
427 modeling of organic acid production in the troposphere has proven helpful in understanding how
428 VOC emissions are transformed into organic acids and transported to Whiteface Mountain in
429 New York (Lawrence et al. 2024). Similar modeling focused on the HBEF during the 2000-2020
430 increase in DOC bulk deposition could help address hypotheses related to changing oxidation
431 potential or pathways in the troposphere. Additionally, modeling BVOC forest emissions would
432 help us test whether forest warming or other environmental changes would be predicted to in-
433 crease BVOC emissions, as has been applied globally (Shen et al. 2019; Wang et al. 2024). Re-
434 mote sensing data of atmospheric BVOCs concentrations should be explored to see if they sup-
435 port the hypothesis that BVOC emissions have increased suddenly and the spatial extent of any
436 increase (Wells et al. 2022). Finally, more long-term observations of DOC deposition are needed
437 to understand changes like we observed. DOC is not often included as an analyte in atmospheric
438 deposition monitoring; adding it could contribute better information about the changing organic
439 chemistry of the troposphere.

440

441 Conclusion

442 We observed a sudden doubling of DOC concentration of precipitation between 2010 and 2022
443 at the HBEF that was not associated with changes in concentrations of other solutes or air mass
444 trajectory changes. Given the available evidence, we hypothesize that the increase in precipita-
445 tion DOC concentration was primarily due to either an increase in BVOC emissions from the
446 forest at the HBEF, since this would cause an increase in DOC but not other solutes, or an in-
447 crease in dissolution of gas phase organic carbon due to higher pH and lower nitrogen concentra-
448 tions. Given other, recent changes at the HBEF associated with sudden changes in the carbon cy-
449 cle, we further hypothesize that an increase in BVOC emissions could be caused by an increase
450 in forest photosynthesis or a heat stress response to recent increases in late summer and early au-
451 tumn air temperatures. These hypotheses warrant further investigation.

452

453 Open Research

454 All data used in this analysis are publicly available. Precipitation bulk deposition chemistry data
455 are available at the Environmental Data Initiative (Hubbard Brook Watershed Ecosystem Record
456 2004). Water vapor pressure data are available at the Environmental Data Initiative (USDA For-
457 est Service 2023). Daily and 15-minute precipitation data are available at the Environmental
458 Data Initiative (USDA Forest Service 2024a, 2024b). Ozone and nitrogen dry deposition are
459 available through the CASTNET Network (U.S. Environmental Protection Agency 2024). Wet
460 deposition data are available through the National Atmospheric Deposition Program (NADP
461 2022).

462

463 References

464

465 Allen, A. G., & Miguel, A. H. (1995). Biomass burning in the Amazon: Characterization of the
466 ionic component of aerosols generated from flaming and smoldering rainforest and savannah.
467 *Environmental Science & Technology*, 29(2), 486-493.

468

469 Anglada, J. M., Crehuet, R., Martins-Costa, M., Francisco, J. S., & Ruiz-López, M. (2017). The
470 atmospheric oxidation of CH₃OOH by the OH radical: the effect of water vapor. *Physical
471 Chemistry Chemical Physics*, 19(19), 12331-12342.

472

473 Baldocchi, D., Guenther, A., Harley, P., Klinger, L., Zimmerman, P., Lamb, B., & Westberg, H.
474 (1995). The fluxes and air chemistry of isoprene above a deciduous hardwood forest. *Philosophical Transactions of the Royal Society of London. Series A: Physical and Engineering Sciences*,
475 351(1696), 279-296.

477

478 Bloomer, B. J., Vinnikov, K. Y., & Dickerson, R. R. (2010). Changes in seasonal and diurnal cy-
479 cles of ozone and temperature in the eastern US. *Atmospheric Environment*, 44(21-22), 2543-
480 2551.

481

482 Boyer, E. W., Moritz, M. A., & Brown, M. G. (2022). Smoke deposition to water surfaces drives
483 hydrochemical changes. *Hydrological Processes*, 36(6), e14626.

484

485 Brahney, J., Ballantyne, A. P., Sievers, C., & Neff, J. C. (2013). Increasing Ca²⁺ deposition in
486 the western US: The role of mineral aerosols. *Aeolian Research*, 10, 77-87.

487

488 Buso, D. C., Likens, G. E., & Eaton, J. S. (2000). *Chemistry of precipitation, streamwater, and
489 lakewater from the Hubbard Brook Ecosystem Study: a record of sampling protocols and analyt-
490 ical procedures*. <http://dx.doi.org/10.2737/NE-GTR-275>

491

492 Campbell, J. L., Rustad, L. E., Bailey, S. W., Bernhardt, E. S., Driscoll, C. T., Green, M. B.,
493 Groffman, P. M., Lovett, G. M., McDowell, W. H., McGuire, K. J., & Rosi, E. J. (2021). Water-
494 shed studies at the Hubbard Brook Experimental Forest: Building on a long legacy of research
495 with new approaches and sources of data. *Hydrological Processes*, 35(1), e14016.

496 <https://doi.org/https://doi.org/10.1002/hyp.14016>

497

498 Cao, J., Pan, Y., Yu, S., Zheng, B., Ji, D., Hu, J., & Liu, J. (2022). Rapid decline in atmospheric
499 organic carbon deposition in rural Beijing, North China between 2016 and 2020. *Atmospheric
500 Environment*, 276, 119030.

501

502 Ciccioli, P., Centritto, M., & Loreto, F. (2014). Biogenic volatile organic compound emissions
503 from vegetation fires. *Plant, Cell & Environment*, 37(8), 1810-1825.

504

505 Clarke, J. F., Edgerton, E. S., & Martin, B. E. (1997). Dry deposition calculations for the clean
506 air status and trends network. *Atmospheric Environment*, 31(21), 3667-3678.

507

508 Cui, L., Song, X., & Zhong, G. (2021). Comparative analysis of three methods for HYSPLIT at-
509 mospheric trajectories clustering. *Atmosphere*, 12(6), 698.

510

511 DeBell, L. J., Talbot, R. W., Dibb, J. E., Munger, J. W., Fischer, E. V., & Frolking, S. E. (2004).
512 A major regional air pollution event in the northeastern United States caused by extensive forest
513 fires in Quebec, Canada. *Journal of Geophysical Research: Atmospheres*, 109(D19).

514

515 de Gouw, J. A., Warneke, C., Stohl, A., Wollny, A. G., Brock, C. A., Cooper, O. R., ... & Lueb,
516 A. (2006). Volatile organic compounds composition of merged and aged forest fire plumes from
517 Alaska and western Canada. *Journal of Geophysical Research: Atmospheres*, 111(D10).

518

519 de Vicente, I., Ortega-Retuerta, E., Morales-Baquero, R., & Reche, I. (2012). Contribution of
520 dust inputs to dissolved organic carbon and water transparency in Mediterranean reservoirs. *Bio-
521 geosciences*, 9(12), 5049-5060.

522

523 Dube, K. A., McDonald, D. G., & O'Donnell, M. J. (2000). Calcium homeostasis in larval and
524 adult *Drosophila melanogaster*. *Archives of Insect Biochemistry and Physiology*: Published in
525 Collaboration with the Entomological Society of America, 44(1), 27-39.

526

527 Evans, J. S., Norman, A. L., & Reid, M. L. (2021). Evidence of smoke from wildland fire in sur-
528 face water of an unburned watershed. *Water Resources Research*, 57(10), e2021WR030069.

529

530 Fahey, T. J., Siccama, T. G., Driscoll, C. T., Likens, G. E., Campbell, J., Johnson, C. E., ... &
531 Yanai, R. D. (2005). The biogeochemistry of carbon at Hubbard Brook. *Biogeochemistry*, 75,
532 109-176.

533

534 Ferracci, V., Bolas, C. G., Freshwater, R. A., Staniaszek, Z., King, T., Jaars, K., ... & Harris, N.
535 R. (2020). Continuous isoprene measurements in a UK temperate forest for a whole growing sea-
536 son: Effects of drought stress during the 2018 heatwave. *Geophysical Research Letters*, 47(15),
537 e2020GL088885.

538

539 Fuss, C. B., Driscoll, C. T., & Campbell, J. L. (2015). Recovery from chronic and snowmelt
540 acidification: Long-term trends in stream and soil water chemistry at the Hubbard Brook Experi-
541 mental Forest, New Hampshire, USA. *Journal of Geophysical Research: Biogeosciences*,
542 120(11), 2360-2374.

543

544 Ghimire, R. P., Silfver, T., Myller, K., Oksanen, E., Holopainen, J. K., & Mikola, J. (2022).
545 BVOC emissions from a subarctic ecosystem, as controlled by insect herbivore pressure and
546 temperature. *Ecosystems*, 25(4), 872-891.

547

548 Green, M. B., Campbell, J. L., Yanai, R. D., Bailey, S. W., Bailey, A. S., Grant, N., Halm, I.,
549 Kelsey, E. P., & Rustad, L. E. (2018). Downsizing a long-term precipitation network: Using a
550 quantitative approach to inform difficult decisions. *PLoS One*, 13(5), e0195966.
551 <https://doi.org/10.1371/journal.pone.0195966>

552

553 Green, M. B., Bailey, S. W., Campbell, J. L., McGuire, K. J., Bailey, A. S., Fahey, T. J., ... &
554 Zietlow, D. (2021). A catchment water balance assessment of an abrupt shift in evapotranspiration at the Hubbard Brook Experimental Forest, New Hampshire, USA. *Hydrological Processes*,
555 35(8), e14300.

557

558 Guenther, A., Karl, T., Harley, P., Wiedinmyer, C., Palmer, P. I., & Geron, C. (2006). Estimates
559 of global terrestrial isoprene emissions using MEGAN (Model of Emissions of Gases and Aero-
560 sols from Nature). *Atmospheric Chemistry and Physics*, 6(11), 3181-3210.

561

562 Harley, P. C., Monson, R. K., & Lerdau, M. T. (1999). Ecological and evolutionary aspects of
563 isoprene emission from plants. *Oecologia*, 118, 109-123.

564

565 Helmig, D., Klinger, L. F., Guenther, A., Vierling, L., Geron, C., & Zimmerman, P. (1999). Biogenic volatile organic compound emissions (BVOCs) I. Identifications from three continental
566 sites in the US. *Chemosphere*, 38(9), 2163-2187.

568

569 Hubbard Brook Watershed Ecosystem Record (HBWatER). 2024. Continuous precipitation and
570 stream chemistry data, Hubbard Brook Ecosystem Study, 1963 – ongoing. ver 11. Environmental
571 Data Initiative. <https://doi.org/10.6073/pasta/3e4b95149245341d522383bba51de7c7> (Accessed
572 2024-06-16).

573

574 Hughes, J. W., & Fahey, T. J. (1991). Colonization dynamics of herbs and shrubs in a disturbed
575 northern hardwood forest. *The Journal of Ecology*, 605-616.

576

577 Iavorivska, L., Boyer, E. W., & DeWalle, D. R. (2016). Atmospheric deposition of organic carbon
578 via precipitation. *Atmospheric Environment*, 146, 153-163.

579

580 Kalnay, E., Kanamitsu, M., Kistler, R., Collins, W., Deaven, D., Gandin, L., Iredell, M., Saha,
581 S., White, G., & Woollen, J. (2018). The NCEP/NCAR 40-year reanalysis project. In *Renewable
582 energy* (pp. Vol1_146-Vol141_194). Routledge.

583

584 Harrison, J. L., Blagden, M., Green, M. B., Salvucci, G. D., & Templer, P. H. (2020). Water
585 sources for red maple trees in a northern hardwood forest under a changing climate. *Ecohydrology*,
586 13(8), e2248.

587

588 Hartigan, J. A., & Wong, M. A. (1979). A k-means clustering algorithm. *Applied Statistics*,
589 28(1), 100-108.

590

591 Heald, C. L., Goldstein, A. H., Allan, J. D., Aiken, A. C., Apel, E., Atlas, E. L., ... & Zheng, W.
592 (2008). Total observed organic carbon (TOOC) in the atmosphere: a synthesis of North Ameri-
593 can observations. *Atmospheric Chemistry and Physics*, 8(7), 2007-2025.

594

595 Heald, C. L., & Kroll, J. H. (2020). The fuel of atmospheric chemistry: Toward a complete de-
596 scription of reactive organic carbon. *Science Advances*, 6(6), eaay8967.

597

598 Huang, J.; Kang, S.; Shen, C.; Cong, Z.; Liu, K.; Wang, W.; Liu, L. Seasonal variations and
599 sources of ambient fossil and biogenic-derived carbonaceous aerosols based on ^{14}C measure-
600 ments in Lhasa, Tibet. *Atmos. Res.*; 2010; 96, pp. 553-559. [DOI: <https://dx.doi.org/10.1016/j.atmosres.2010.01.003>]

602

603 Khare, P., Kumar, N., Kumari, K. M., & Srivastava, S. S. (1999). Atmospheric formic and acetic
604 acids: An overview. *Reviews of Geophysics*, 37(2), 227-248.

605

606 Lamb, D., & Bowersox, V. (2000). The national atmospheric deposition program: an overview.
607 *Atmospheric Environment*, 34(11), 1661-1663.

608

609 Lantz, A. T., Allman, J., Weraduwage, S. M., & Sharkey, T. D. (2019). Control of rate and phys-
610 iological role of isoprene emission from plants. *Plant, Cell & Environment*, 42(10), 2808.

611

612 Lany, N. (2024). Digitized 15-minute resolution precipitation dataset for rain gauge 1 in the Hub-
613 bard Brook Experimental Forest, 1956 - 2011.

614

615 Lawrence, C. E., Casson, P., Brandt, R., Schwab, J. J., Dukett, J. E., Snyder, P., ... & Lance, S.
616 (2023). Long-term monitoring of cloud water chemistry at Whiteface Mountain: the emergence
617 of a new chemical regime. *Atmospheric Chemistry and Physics*, 23(2), 1619-1639.

618

619 Lawrence, C., Barth, M., Orlando, J., Casson, P., Brandt, R., Kelting, D., ... & Lance, S. (2024).
620 Process analysis of elevated concentrations of organic acids at Whiteface Mountain, New York.
621 *Atmospheric Chemistry and Physics*, 24(23), 13693-13713.

622

623 Lee, E. J., Kenkel, N., & Booth, T. (1996). Atmospheric deposition of macronutrients by pollen
624 in the boreal forest. *Ecoscience*, 3(3), 304-309.

625

626 Lelieveld, J., Gromov, S., Pozzer, A., & Taraborrelli, D. (2016). Global tropospheric hydroxyl
627 distribution, budget and reactivity. *Atmospheric Chemistry and Physics*, 16(19), 12477-12493.
628

629 Li, C.; Yan, F.; Kang, S.; Chen, P.; Qu, B.; Hu, Z.; Sillanpää, M. Concentration, sources, and
630 flux of dissolved organic carbon of precipitation at Lhasa city, the Tibetan Plateau. *Environ. Sci.
631 Pollut. Res.*; 2016; 23, pp. 12915-12921. [DOI: <https://dx.doi.org/10.1007/s11356-016-6455-1>]

632

633 Likens, G. E., Edgerton, E. S., & Galloway, J. N. (1983). The composition and deposition of or-
634 ganic carbon in precipitation 1. *Tellus B*, 35(1), 16-24.

635

636 Link, M. F., Nguyen, T. B., Bates, K., Müller, J. F., & Farmer, D. K. (2020). Can isoprene oxidation explain high concentrations of atmospheric formic and acetic acid over forests? *ACS Earth and Space Chemistry*, 4(5), 730-740.

639

640 Link, M. F., Brophy, P., Fulgham, S. R., Murschell, T., & Farmer, D. K. (2021). Isoprene versus 641 monoterpenes as gas-phase organic acid precursors in the atmosphere. *ACS Earth and Space 642 Chemistry*, 5(6), 1600-1612.

643

644 Liptzin, D., Boy, J., Campbell, J. L., Clarke, N., Laclau, J. P., Godoy, R., ... & McDowell, W. H. 645 (2022). Spatial and temporal patterns in atmospheric deposition of dissolved organic carbon. 646 *Global Biogeochemical Cycles*, 36(10), e2022GB007393.

647

648 Liu, L., Liu, X., Zhang, Y., & Yang, W. (2017). Effects of land use on dissolved organic matter 649 in precipitation in a rapidly urbanizing area. *Environmental Pollution*, 224, 247-256.

650

651 Mann, T. A., Yanai, R. D., Fahey, T. J., & Reinmann, A. B. (2024). Nitrogen and phosphorus addition 652 affect soil respiration in Northern Hardwood Forests. *Ecosystems*, 1-14.

653

654 Martin, C. W., Likens, G. E., & Buso, D. C. (2000). Comparison of long-term precipitation 655 chemistry measurements at the Hubbard Brook Experimental Forest, New Hampshire. *Water, Air, and Soil Pollution*, 120, 359-379.

657

658 Mead, R. N., Mullaugh, K. M., Brooks Avery, G., Kieber, R. J., Willey, J. D., & Podgorski, D. 659 C. (2013). Insights into dissolved organic matter complexity in rainwater from continental and 660 coastal storms by ultrahigh resolution Fourier transform ion cyclotron resonance mass spectrometry. *Atmospheric Chemistry and Physics*, 13(9), 4829-4838.

662

663 McKinney, K. A., Lee, B. H., Vasta, A., Pho, T. V., & Munger, J. W. (2011). Emissions of isoprenoids and oxygenated biogenic volatile organic compounds from a New England mixed forest. *Atmospheric Chemistry and Physics*, 11(10), 4807-4831.

666

667 Monson, R. K., Winkler, B., Rosenstiel, T. N., Block, K., Merl-Pham, J., Strauss, S. H., ... & 668 Schnitzler, J. P. (2020). High productivity in hybrid-poplar plantations without isoprene emission 669 to the atmosphere. *Proceedings of the National Academy of Sciences*, 117(3), 1596-1605.

670

671 Muggeo VMR (2016). Testing with a nuisance parameter present only under the alternative: a 672 score-based approach with application to segmented modelling. *J of Statistical Computation and 673 Simulation*, 86, 3059-3067.

674

675 National Atmospheric Deposition Program (NRSP-3). (2022). NADP Program Office, Wisconsin State Laboratory of Hygiene, 465 Henry Mall, Madison, WI 53706,
676
677 <https://nadp.slh.wisc.edu/>.

678

679 Nguyen, T. B., Crounse, J. D., Teng, A. P., St. Clair, J. M., Paulot, F., Wolfe, G. M., & Wennberg, P. O. (2015). Rapid deposition of oxidized biogenic compounds to a temperate forest. *Proceedings of the National Academy of Sciences*, 112(5), E392-E401.

682

683 Paulot, F., Crounse, J. D., Kjaergaard, H. G., Kürten, A., St. Clair, J. M., Seinfeld, J. H., & Wennberg, P. O. (2009). Unexpected epoxide formation in the gas-phase photooxidation of isoprene. *Science*, 325(5941), 730-733.

686

687 Pebesma, E., 2018. Simple Features for R: Standardized Support for Spatial Vector Data. The R Journal 10 (1), 439-446, <https://doi.org/10.32614/RJ-2018-009>

689

690 Pebesma E (2021). lwgeom: Bindings to Selected 'liblwgeom' Functions for Simple Features. R package version 0.2-8, <<https://CRAN.R-project.org/package=lwgeom>>.

692

693 Pebesma, E., & Bivand, R. (2023). Spatial Data Science: With Applications in R. Chapman and Hall/CRC. <https://doi.org/10.1201/9780429459016>

695

696 Possinger, A., C. Driscoll, T. Fahey, M. Green, P. Groffman, C. Johnson, L. Martel, J. Morse, P. Templer, G. Wilson. (2005) Symptoms of a Changing Carbon Cycle: a Breakpoint Increase in Soil Respiration in a Northern Hardwood Forest. *Nature Communications*.

699

700 Raymond, P. A. (2005). The composition and transport of organic carbon in rainfall: Insights from the natural (13C and 14C) isotopes of carbon. *Geophysical Research Letters*, 32(14).

702

703 Richardson, A. D., Bailey, A. S., Denny, E. G., Martin, C. W., & O'KEEFE, J. O. H. N. (2006). Phenology of a northern hardwood forest canopy. *Global Change Biology*, 12(7), 1174-1188.

705

706 Rösel, S., Rychła, A., Wurzbacher, C., & Grossart, H. P. (2012). Effects of pollen leaching and microbial degradation on organic carbon and nutrient availability in lake water. *Aquatic sciences*, 708 74, 87-99.

709

710 Saarikoski, S., Timonen, H., Saarnio, K., Aurela, M., Järvi, L., Keronen, P., ... & Hillamo, R. (2008). Sources of organic carbon in fine particulate matter in northern European urban air. *Atmospheric Chemistry and Physics*, 8(20), 6281-6295.

713

714 Safieddine, S. A., & Heald, C. L. (2017). A global assessment of dissolved organic carbon in
715 precipitation. *Geophysical Research Letters*, 44(22), 11-672.
716

717 Schaefer, D. A., Lindberg, S. E., & Hoffman Jr, W. A. (1989). Fluxes of undissociated acids to
718 terrestrial ecosystems by atmospheric deposition. *Tellus B*, 41(3), 207-218.
719

720 Schollert, M., Kivimäenpää, M., Michelsen, A., Blok, D., & Rinnan, R. (2017). Leaf anatomy,
721 BVOC emission and CO₂ exchange of arctic plants following snow addition and summer warm-
722 ing. *Annals of Botany*, 119(3), 433-445.
723

724 Shen, H., Chen, Y., Li, Y., Russell, A. G., Hu, Y., Henneman, L. R., ... & Driscoll, C. T. (2019).
725 Relaxing energy policies coupled with climate change will significantly undermine efforts to at-
726 tain US ozone standards. *One Earth*, 1(2), 229-239.
727

728 Shrivastava, M., et al. (2017), Recent advances in understanding secondary organic aerosol: Im-
729 plications for global climate forcing, *Rev. Geophys.*, 55, 509–559, doi:[10.1002/2016RG000540](https://doi.org/10.1002/2016RG000540).
730

731 Sindelarova, K., Granier, C., Bouarar, I., Guenther, A., Tilmes, S., Stavrakou, T., ... & Knorr, W.
732 (2014). Global data set of biogenic VOC emissions calculated by the MEGAN model over the
733 last 30 years. *Atmospheric Chemistry and Physics*, 14(17), 9317-9341.
734

735 Siudek, P., Frankowski, M., & Siepak, J. (2015). Seasonal variations of dissolved organic carbon
736 in precipitation over urban and forest sites in central Poland. *Environmental Science and Pollu-
737 tion Research*, 22, 11087-11096.
738

739 Stein, A.F., Draxler, R.R, Rolph, G.D., Stunder, B.J.B., Cohen, M.D., and Ngan, F., (2015).
740 NOAA's HYSPLIT atmospheric transport and dispersion modeling system, Bull. Amer. Meteor.
741 Soc., 96, 2059-2077, <http://dx.doi.org/10.1175/BAMS-D-14-00110.1>
742

743 Sun, J., & Ariya, P. A. (2006). Atmospheric organic and bio-aerosols as cloud condensation nu-
744 clei (CCN): A review. *Atmospheric Environment*, 40(5), 795-820.
745

746 Tagesson, T., Kelly, J., Schurgers, G., Tian, F., Ardö, J., Horion, S., ... & Fensholt, R. (2024).
747 Increasing global ecosystem respiration between 1982 and 2015 from Earth observation-based
748 modelling. *Global Ecology and Biogeography*, 33(1), 116-130.
749

750 USDA Forest Service, Northern Research Station. 2019. USFS Durham Lab water analysis
751 method detection limit (MDL) limit of quantification (LOQ), 2010 - present ver 1. Environmen-
752 tal Data Initiative. <https://doi.org/10.6073/pasta/890b1fadb61d3e86dc6f3d9afea79705> (Accessed
753 2025-05-20).
754

755 USDA Forest Service, Northern Research Station. 2024a. Hubbard Brook Experimental Forest:
756 Daily Precipitation Rain Gage Measurements, 1956 - present ver 21. Environmental Data Initiative.
757 <https://doi.org/10.6073/pasta/780d9eabe5e0e40fcb1ab44a34210e38> (Accessed 2023-03-01).
758

759 USDA Forest Service, Northern Research Station. 2023. Hubbard Brook Experimental Forest
760 (USDA Forest Service): Vapor Pressure Measurements, 1966 - present ver 10. Environmental
761 Data Initiative. <https://doi.org/10.6073/pasta/c3a8d64d96a3dbb8edebf1c9f23bcd5f> (Accessed
762 2024-07-26).
763

764 USDA Forest Service, Northern Research Station. 2024b. Hubbard Brook Experimental Forest:
765 15-minute Precipitation Measurements, 2011 - present ver 9. Environmental Data Initiative.
766 <https://doi.org/10.6073/pasta/ea069a2227869426d82b15b573343688> (Accessed 2024-07-26).
767

768 U.S. Environmental Protection Agency. 2024. Clean Air Markets Division, Clean Air Status and
769 Trends Network (CASTNET). Hourly Ozone and Dry Deposition. Available at
770 www.epa.gov/castnet, Date accessed: October 2024.
771

772 U.S. EPA, 2023. National Emission Inventory Emissions trends report <https://www.epa.gov/air-emissions-inventories/air-pollutant-emissions-trends-data>.
773

774 Wang, H., Liu, X., Wu, C., & Lin, G. (2024). Regional to global distributions, trends, and drivers
775 of biogenic volatile organic compound emission from 2001 to 2020. *Atmospheric Chemistry and
776 Physics*, 24(5), 3309-3328.
777

778 Wells, K. C., Millet, D. B., Payne, V. H., Vigouroux, C., Aquino, C. A. B., De Mazière, M., ... &
779 Wisthaler, A. (2022). Next-generation isoprene measurements from space: Detecting daily varia-
780 bility at high resolution. *Journal of Geophysical Research: Atmospheres*, 127(5),
781 e2021JD036181.
782

783 Willey, J. D., Kieber, R. J., Eyman, M. S., & Avery Jr, G. B. (2000). Rainwater dissolved or-
784 ganic carbon: concentrations and global flux. *Global Biogeochemical Cycles*, 14(1), 139-148.
785

786 Willey, J. D., Glinski, D. A., Southwell, M., Long, M. S., Avery Jr, G. B., & Kieber, R. J.
787 (2011). Decadal variations of rainwater formic and acetic acid concentrations in Wilmington,
788 NC, USA. *Atmospheric Environment*, 45(4), 1010-1014.
789

790 Williams, M. W., & Melack, J. M. (1991). Precipitation chemistry in and ionic loading to an al-
791 pine basin, Sierra Nevada. *Water Resources Research*, 27(7), 1563-1574.
792

793

794 Wilson, G., Groffman, P., Martel, L., Green, M. B., Driscoll, C. T., Durán, J., ... & Fisk, M. C.
795 (2025). Changes in soil moisture and its relationships with nitrogen cycle processes in a northern
796 hardwood forest. *Canadian Journal of Forest Research*.

797

798 Yan, G.; Kim, G. Dissolved organic carbon in the precipitation of Seoul, Korea: Implications for
799 global wet depositional flux of fossil-fuel derived organic carbon. *Atmos. Environ.*; 2012; 59, pp.
800 117-124. [DOI: <https://dx.doi.org/10.1016/j.atmosenv.2012.05.044>]

801

802 Yu, S. (2000). Role of organic acids (formic, acetic, pyruvic and oxalic) in the formation of
803 cloud condensation nuclei (CCN): a review. *Atmospheric Research*, 53(4), 185-217.

804

805 Zheng, Y., Shen, R., Wang, Y., Li, X., Liu, S., Liang, S., ... & Yuan, W. (2020). Improved esti-
806 mate of global gross primary production for reproducing its long-term variation, 1982–2017.

807 *Earth System Science Data*, 12(4), 2725-2746.

808

809

810 **Acknowledgments**

811 Tammy Wooster collected and processed the routine weekly precipitation chemistry samples.

812 Jeff Merriam and Samantha Auger performed laboratory analyses. Support for this research was
813 provided by the National Science Foundation through the Long Term Research in Environmental
814 Biology (LTREB; DEB-1907683) program, Long Term Ecological Research network (LTER;
815 DEB-1637685), and USDA Forest Service. The Hubbard Brook Experimental Forest is operated
816 and maintained by the USDA Forest Service, Northern Research Station, Madison, WI, USA.

817

818

819 **Table**

820 **Table 1.** Summary of trends in the annual growing season (April to October) volume
 821 weighted concentration from 1996 to 2023 using the Kendall trend test, and the
 822 Spearman correlation between solutes and DOC. Bolded values indicate a significant
 823 result at the $\alpha=0.05$ level.

824

Solute	Temporal Trend		Correlation with DOC
	Kendall τ	Spearman ρ	
Ca ²⁺	0.02	0.37	
Mg ²⁺	-0.00	0.30	
K ⁺	0.07	0.30	
Na ⁺	0.36	0.63	
H ⁺	-0.87	-0.43	
NH ₄ ⁺	-0.45	-0.09	
SO ₄ ²⁻	-0.85	-0.47	
NO ₃ ⁻	-0.66	-0.20	
Cl ⁻	0.45	0.70	
DON	-0.21	-0.23	
DOC	0.36	NA	

825

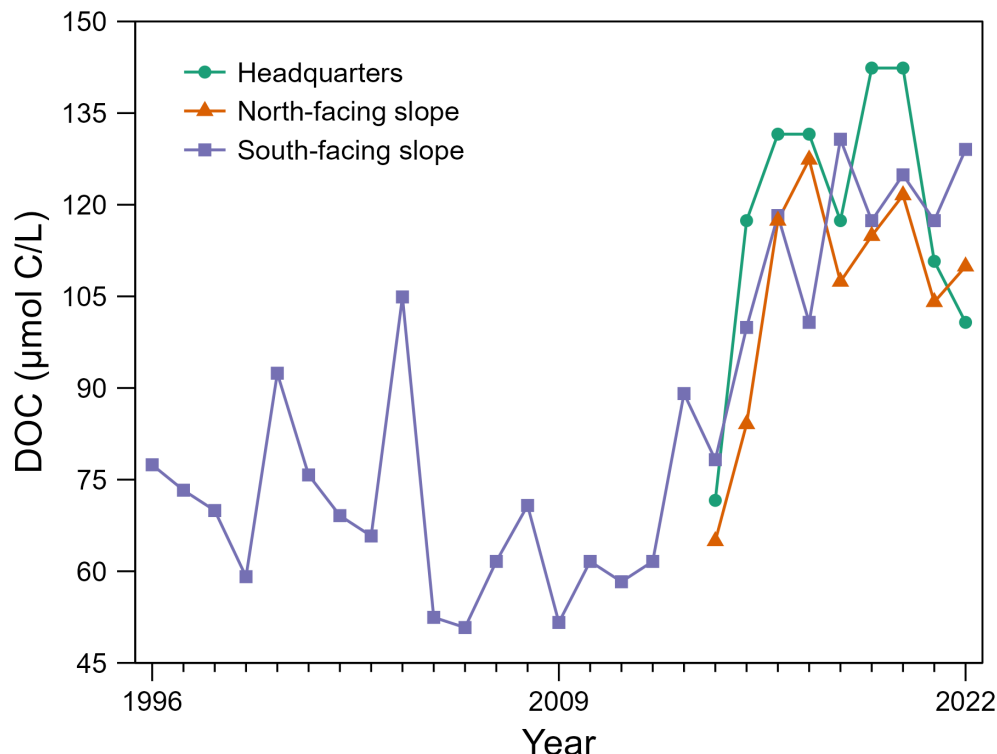
826

827 **Figures**

828

829 **Figure 1.** Mean annual volume-weighted DOC concentration in bulk precipitation at
830 three sites at the Hubbard Brook Experimental Forest. The record from the south-facing
831 slope is from RG1 and RG11, the north-facing slope is from RG23, and from the
832 headquarters site is RG22.

833

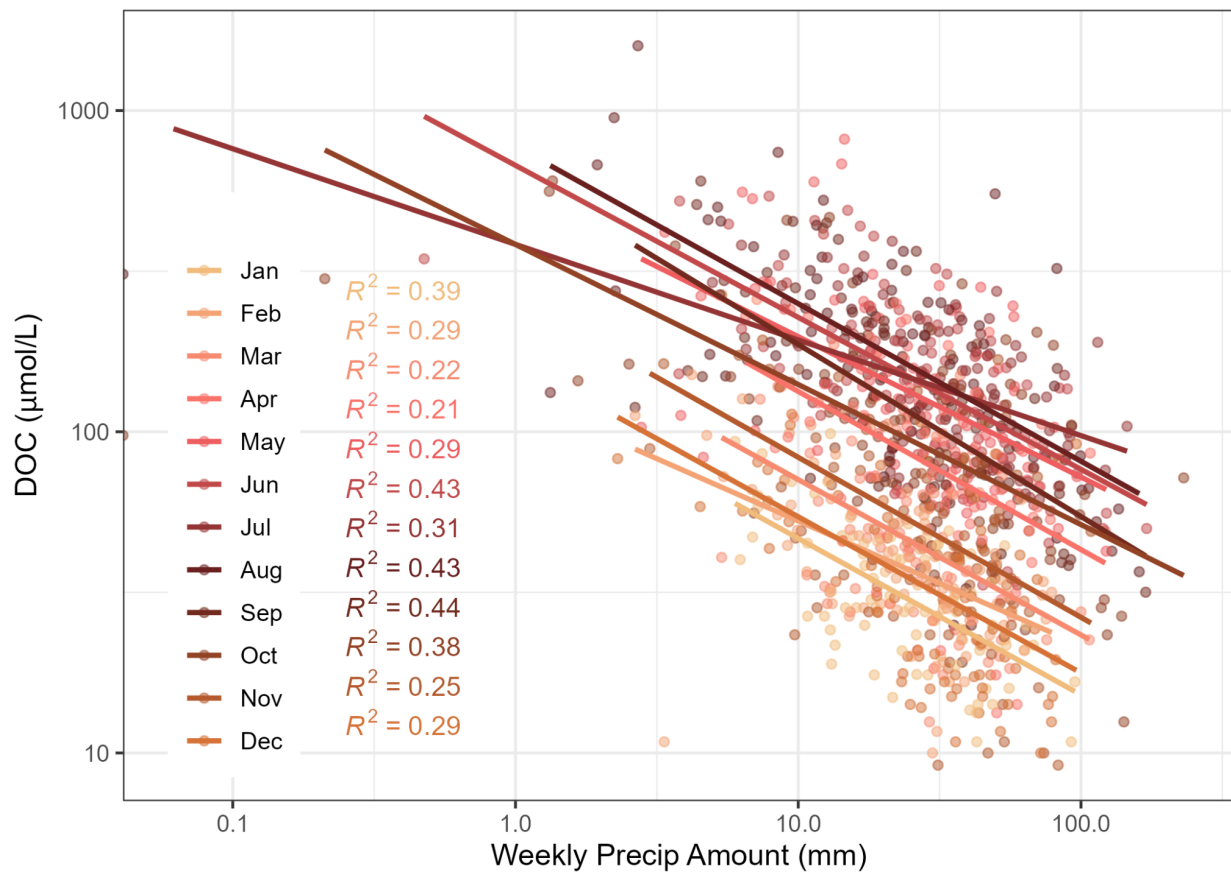


834

835

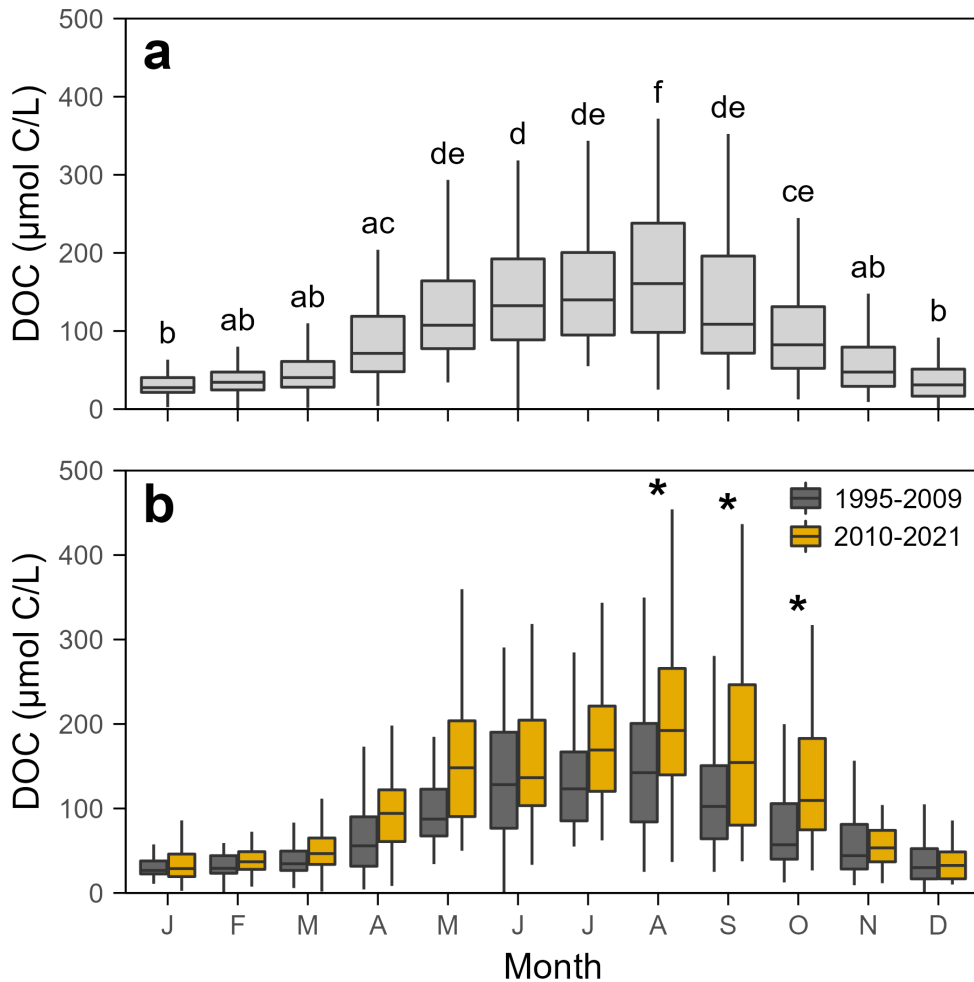
836

837 **Figure 2.** Monthly relationships between bulk precipitation amount and the
838 concentration of DOC on a weekly basis over the period of record at Hubbard Brook.
839



842 **Figure 3.** The seasonality of DOC during the 1995 to 2022 record from the south-facing
843 collectors shows significant monthly differences (panel *a*). The letters above each box in
844 panel *a* indicate the unique group, as indicated by the Tukey HSD *post hoc* test. The
845 data were then split using the 2009 breakpoint in the time series and the months were
846 compared (panel *b*). The stars in panel *b* indicate significant changes before and after
847 2009.

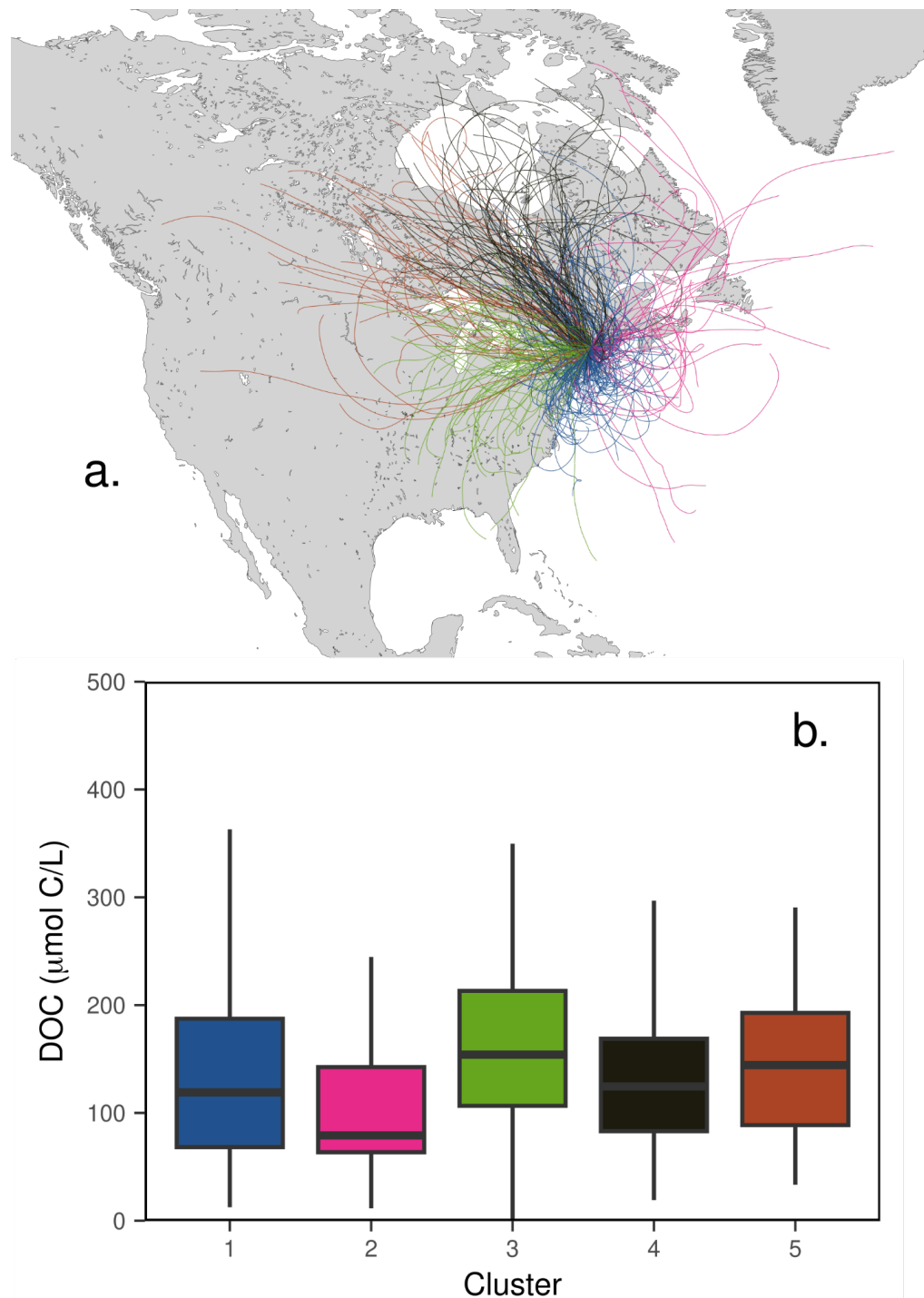
848



849
850

851 **Figure 4.** Air mass trajectories from the HYSPLIT model for April to October storm
852 events (panel a). A comparison of the DOC in these trajectories suggests no difference
853 in their concentrations (ANOVA $p=0.58$; panel b).

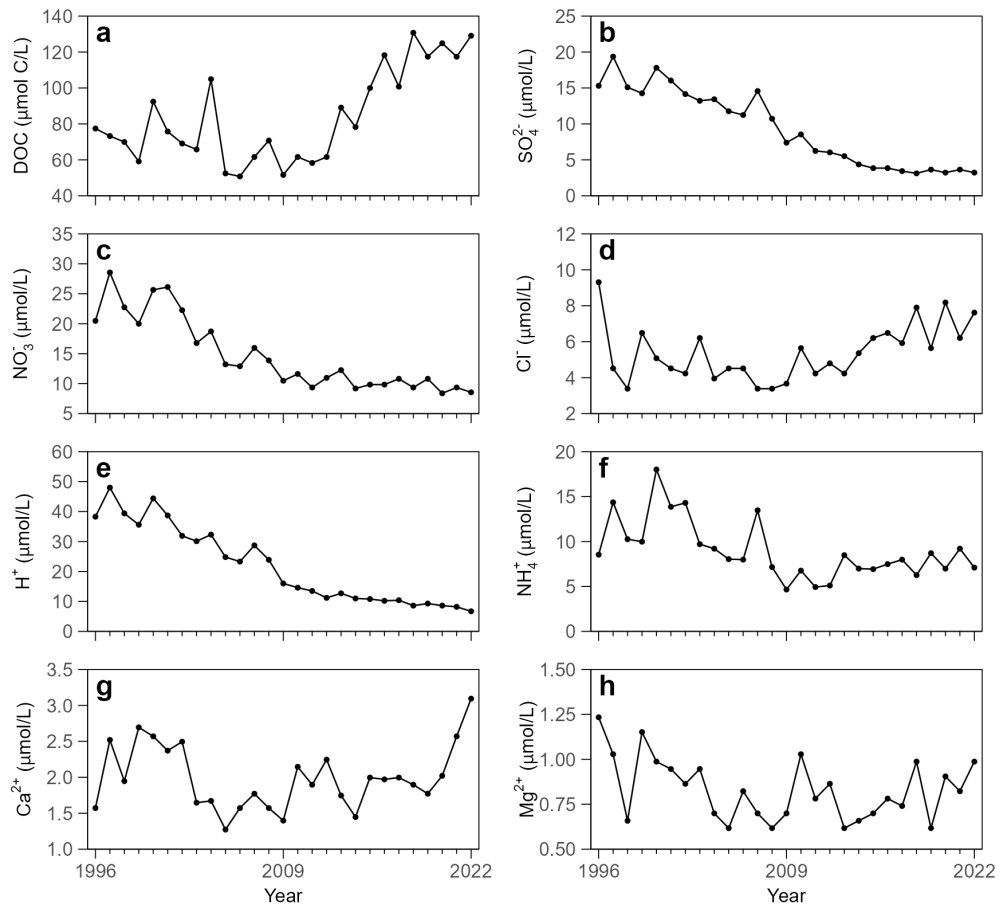
854



855
856

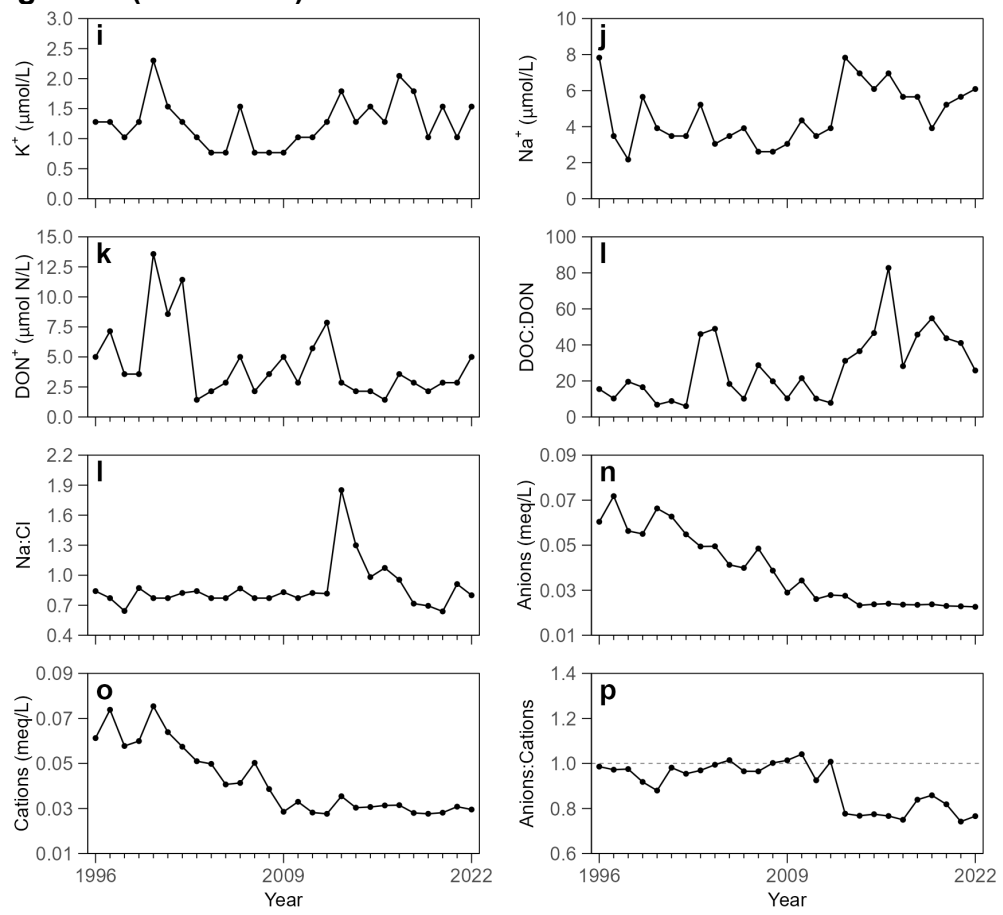
857 **Figure 5.** Mean April to October volume-weighted concentrations of solutes in
 858 precipitation for the collector on the south-facing slope at the Hubbard Brook
 859 Experimental Forest. The ratio of anions to cations (p) is the sum of anions (NO_3^- , SO_4^{2-} ,
 860 Cl^-) divided by the sum of cations (Ca^{2+} , Mg^{2+} , Na^+ , K^+ , H^+ , NH_4^+) calculated in
 861 microequivalents per liter. The $\text{Na}:\text{Cl}$ (panel m) and $\text{DOC}:\text{DON}$ (panel l) ratios are
 862 reported as molar ratios.

863

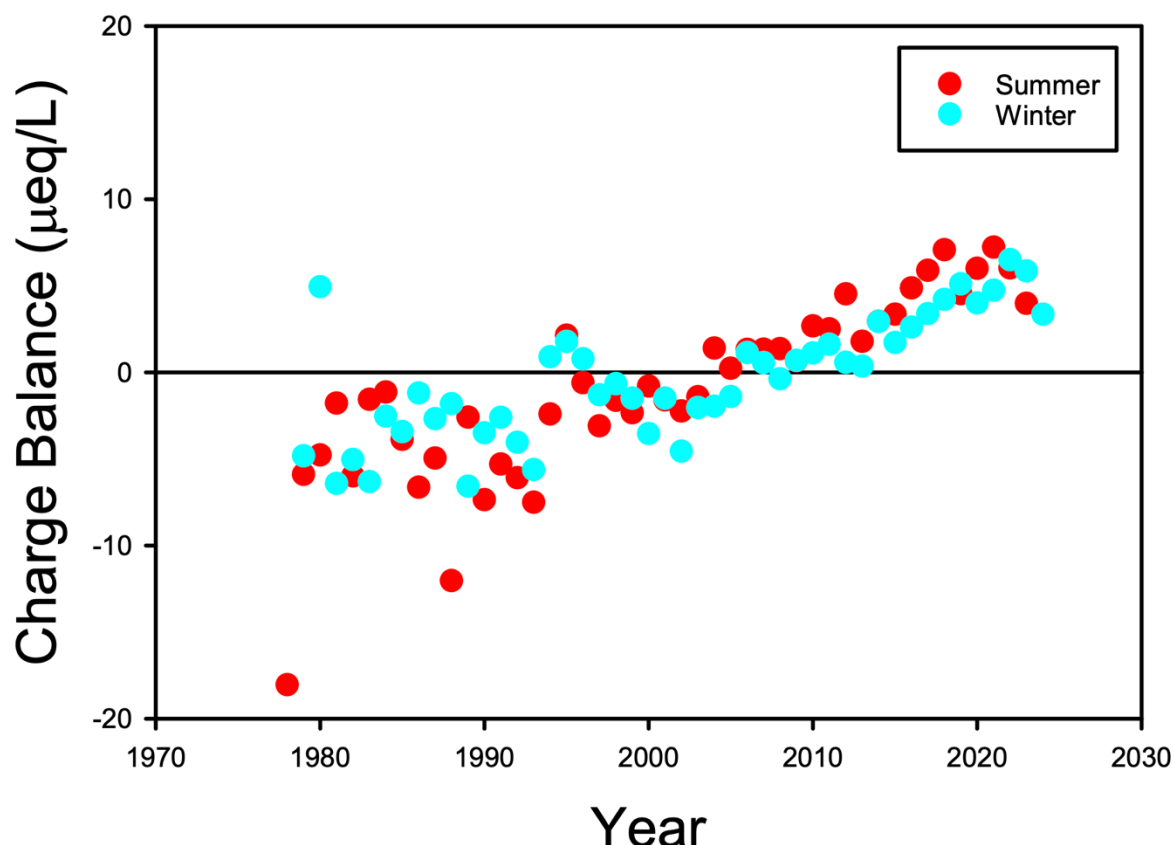


864
 865

866 **Figure 5. (continued)**

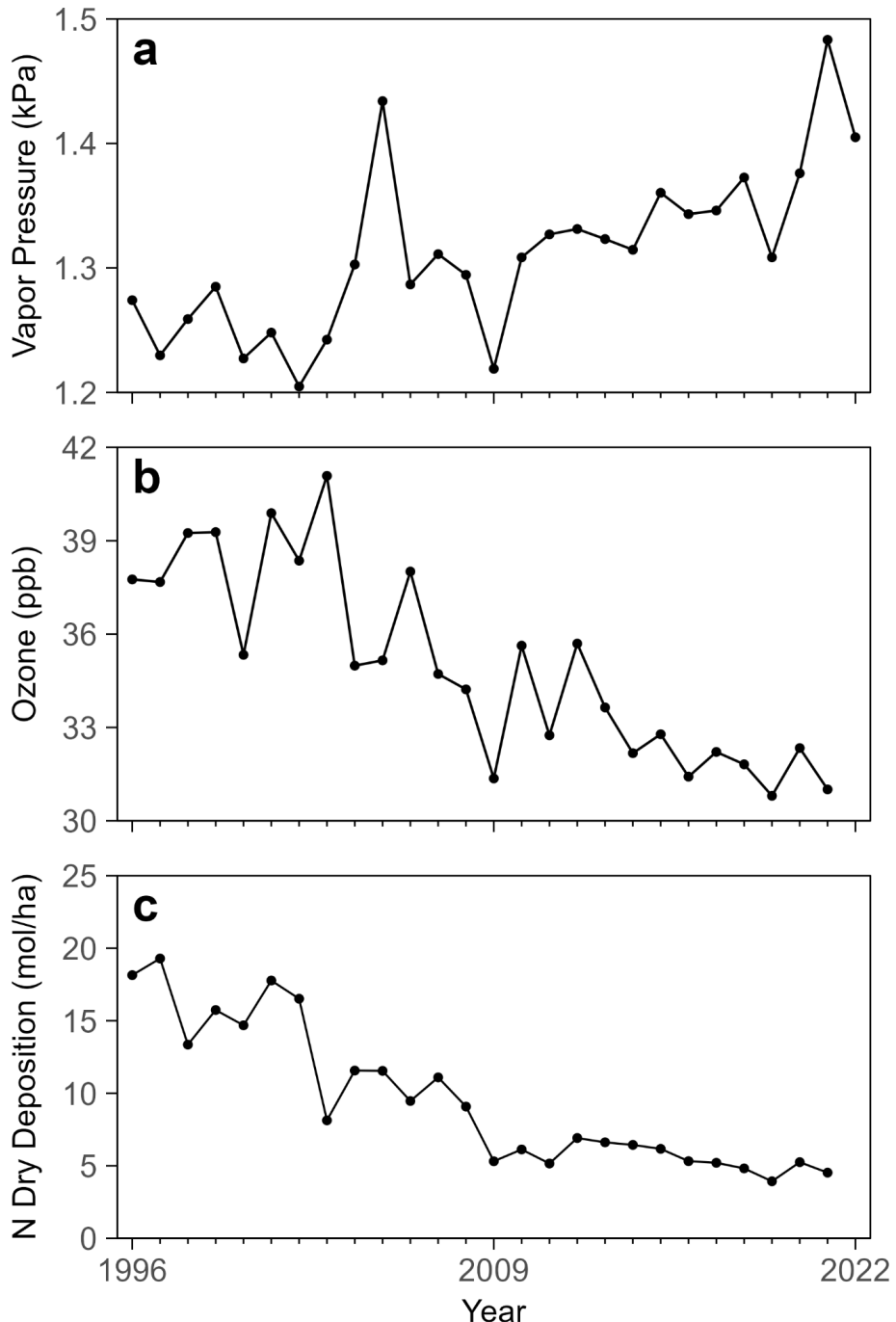


868 **Figure 6.** Change in the charge balance (total cations minus total anions) in wet
869 deposition at Hubbard Brook from the National Atmospheric Deposition Program site.
870 Summer refers to the April to October period and winter is November to March.
871



872
873
874

875 **Figure 7.** Time series of variables that are related to organic matter oxidation in the
876 atmosphere: a) mean water vapor pressure, b) mean ozone, and c) mean dry
877 deposition of reactive N. The mean from April to October, when DOC concentrations are
878 highest, is shown.



879
880

881 **Supplemental Information**

882

883 **Supplemental Methods**

884

885 The mean daily air temperature from three stations at different locations (Stations 1, 14, and 23;)
886 within the Hubbard Brook Experimental Forest were averaged and the mean monthly air temper-
887 ature was calculated and shown in Supplemental Figure 1.

888

889 USDA Forest Service, Northern Research Station. 2024. Hubbard Brook Experimental Forest:

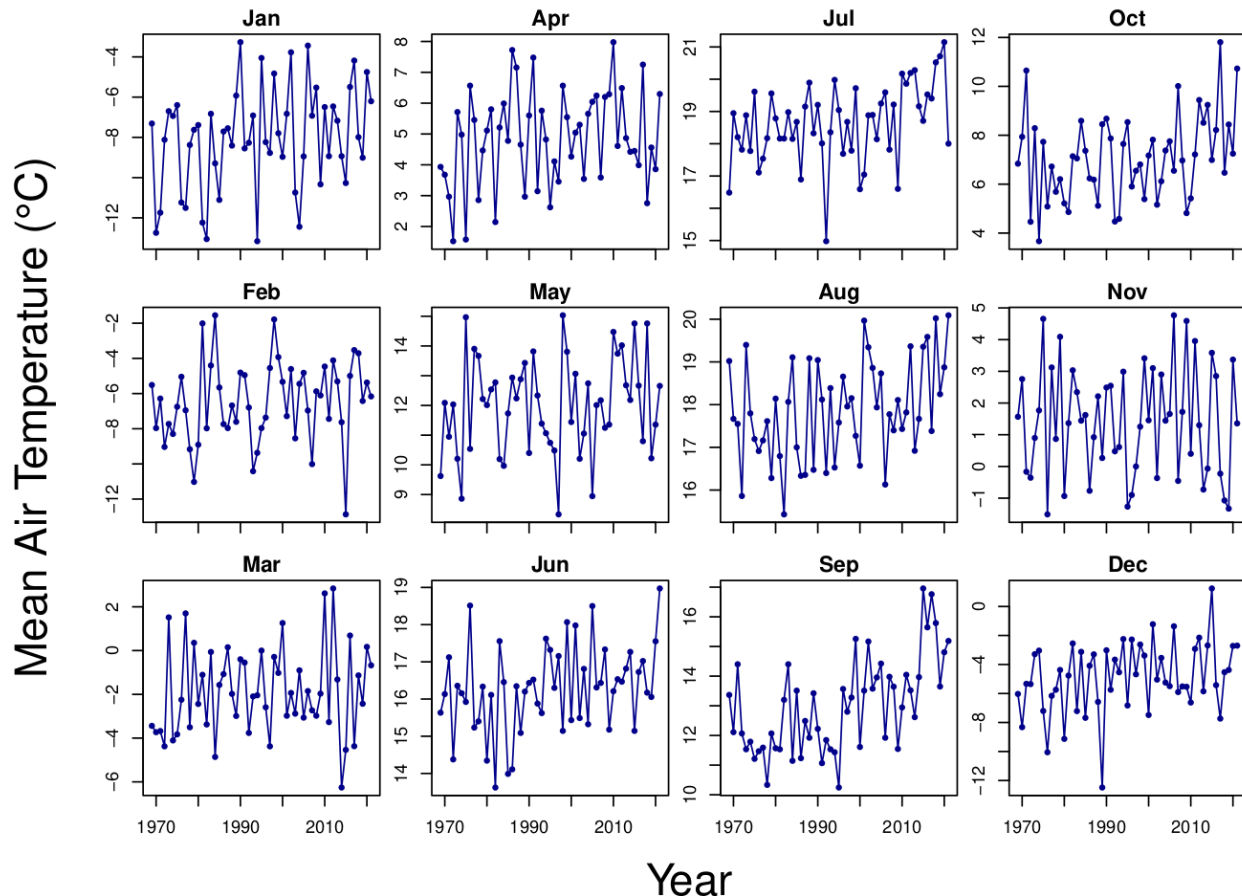
890 Daily Temperature Record, 1955 - present ver 14. Environmental Data Initiative.

891 <https://doi.org/10.6073/pasta/67395641442370b21198973fb553def5>.

892

893

894 **Supplemental Figure 1.** Mean monthly air temperature at the Hubbard Brook Experi-
895 mental Forest.



896

897

898